JMEPEG (2008) 17:543–549
DOI: 10.1007/s11665-007-9161-9

1059-9495/$19.00

Sulfate Attack of Cement-Based Material with Limestone Filler Exposed to Different Environments

Xiaojian Gao, Baoguo Ma, Yingzi Yang, and Anshuang Su

(Submitted January 7, 2007; in revised form July 25, 2007)

Mortar prisms made with OPC cement plus 30% mass of limestone filler were stored in various sulfate solutions at different temperatures for periods of up to 1 year, the visual appearance was inspected at intervals, and the flexural and compressive strength development with immersion time was measured according to the Chinese standard GB/T17671-1999. Samples were selected from the surface of prisms after 1 year immersion and examined by x-ray diffraction (XRD), Fourier transform infrared spectroscopy (FTIR), laser-raman spectroscopy and scanning electron microscopy (SEM). The results show that $MgSO_4$ solution is more aggressive than Na_2SO_4 solution, and Mg^{2+} ions reinforce the thaumasite sulfate attack on the limestone filler cement mortars. The increase of solution temperature accelerates both magnesium attack and sulfate attack on the limestone filler cement mortar, and leads to more deleterious products including gypsum, ettringite and brucite formed on the surface of mortars after 1 year storage in sulfate solutions. Thaumasite forms in the mortars containing limestone filler after exposure to sulfate solutions at both 5 °C and 20 °C. It reveals that the thaumasite form of sulfate attack is not limited to low-temperature conditions.

Keywords cement-based material, limestone filler, sulfate attack, temperature, thaumasite

1. Introduction

The use of limestone aggregates has been common in China and elsewhere for many decades (Ref 1). Especially, in recent years it has become common practice to incorporate fine limestone powder as a minor additional constituent in the cement paste. The European standard allows the use of the term "ordinary Portland cement" with incorporation of up to 5% limestone, while the term "Portland-limestone cement" is used for cements containing 5–35% limestone (Ref 2). A high volume of limestone filler is also used frequently to increase the content of fine particles and optimize the particle packing in self-compacting concrete (SCC) mixes (Ref 3). The use of limestone in cements or concretes seems to have many benefits, such as reducing water demand, improving strength development, and being economical (Ref 4, 5). However, in recent years, it has been widely reported that another kind of sulfate attack, attributed to the formation of thaumasite ($CaSiO_3 \cdot CaCO_3 \cdot CaSO_4 \cdot 15H_2O$), occurs in the cements and concretes containing limestone (Ref 6-8).

Though most researchers believe that thaumasite forms in cool (lower than 15 °C), damp conditions when enough calcium and sulfate ions are available (Ref 6, 9), a few of thaumasite occurrences under warmer conditions have been confirmed by field and lab investigations (Ref 10-12). The literature shows that the pH value and the specific cations (such as Mg^{2+}) present in the sulfate solutions have complicated effects on the formation and stability of thaumasite in cement pastes containing limestone filler (Ref 8, 13), even though there are some conflicting viewpoints on them. Therefore, more work is needed to verify the effects of environments on sulfate attack of limestone filler cements and concretes.

Xiaojian Gao, Yingzi Yang, and **Anshuang Su**, School of Materials Science and Engineering, Harbin Institute of Technology, Harbin 150006, China; and **Baoguo Ma**, Key Laboratory of Silicate Materials Science and Engineering of Ministry of Education, Wuhan University of Technology, Wuhan 430070, China. Contact e-mail: xjgao2002@yahoo.com.cn.

2. Experimental

The cement used is ordinary Portland cement with grade of 42.5 from Huaxin Cement Company of Hubei Province. It has a density of 3.1 g/cm^3 and specific surface area of 350 m^2/kg (Blaine). The limestone from Huangshi City was ground to a specific surface area of 400 m^2/kg (Blaine). The chemical composition of the cement and the limestone are shown in Table 1. A quartz sand was used with a fineness modulus of 2.6 and density of 2.65 g/cm^3. Synthetic $MgSO_4$ and Na_2SO_4 were used to prepare different sulfate solutions.

Mortars based on the materials mentioned above were mixed and cast as 40×40×160-mm prisms. The water to cement ratio was 0.6 and the cement:limestone filler:sand ratio was 1:0.3:2.2. Immediately after molding, the specimens were cured in a moist cabinet for 24 h, removed from the mold, and cured under water for 27 days at room temperature (20 ± 2 °C). After 27 day curing under water, excluding the control specimens (continuously immersed in water), all others were transferred into three different sulfate solutions: (1) 2% $MgSO_4$ solution, (2) 2% Na_2SO_4 solution, and (3) 2% $MgSO_4$ + 2% Na_2SO_4 solution. The solutions were controlled at three different temperatures (with a fluctuation of ±1 °C): (1) 5 °C,

Table 1 Chemical composition of cement and limestone (wt.%)

Name	CaO	SiO_2	Al_2O_3	Fe_2O_3	MgO	SO_3	R_2O	CaO_{free}	IL
Cement	61.27	21.04	6.94	2.36	1.32	1.94	0.97	0.67	3.16
Limestone	51.35	5.63	1.82	0.56	...	...	...	...	40.41

Table 2 Different sulfate solutions and temperatures

Solution No.	Sulfate	Concentration/%	Temperature/°C
M-1	$MgSO_4$	2	5
M-2	$MgSO_4$	2	20
M-3	$MgSO_4$	2	5-20
N-1	Na_2SO_4	2	5
N-2	Na_2SO_4	2	5-20
M + N	Na_2SO_4	2	5
	$MgSO_4$	2	

(2) 20 °C, and (3) cycling temperatures of 5 °C and 20 °C (3 days at each temperature). Therefore, six sulfate environments were provided in the experiment as shown in Table 2. In each case, the sulfate solution was replaced every 2 months and the volume ratio of solution to mortar specimens was kept at about 2:1.

The visual examination and strength measurement were performed on the mortar specimens under different solutions at regular intervals up to 1 year. The visual examination recorded all significant modifications occurring on the specimens, such as changes in surface color and texture, formation of any coatings, deterioration, expansion, and cracking. The mortar strength test was carried out according to the Chinese standard GB/T17671-1999. The flexural strength was measured on three prismatic specimens ($40 \times 40 \times 160$ mm) by means of 3-point bending test as shown in Fig. 1. Then, the compressive strength test was conducted on six pieces of prisms. After the strength test, using the wearing device, layers of 3-mm depth were obtained from the top surfaces of some selected specimens. The material from each layer was collected and sieved through 80 μm sieve to remove the coarse sand grains. Then, the sample was ground to pass through 45 μm sieve and stored in a desiccator to prevent carbonation. Finally, these samples were analyzed by x-ray diffraction (XRD), Fourier transform infrared (FTIR) spectroscopy, laser-raman spectroscopy, and scanning electron microscopy (SEM) to determine changes in mineralogy of the limestone filler cement mortar with continued exposure to different sulfate solutions.

The XRD analysis was conducted using an automated Japan D/MAX-IIIA x-ray diffractometer operating at 35 kV and 30 mA using CuKα radiation. Data was collected between 5° and 60° 2θ using a step-size of 0.02° and a count time of 0.6 s per step. Fourier transform infrared (FTIR) spectroscopy was carried out using a Nicolet 60 SXB FTIR Spectrophotometer. Samples were prepared for analysis by grinding a known mass of solid with dried KBr. The resulting powder was then pressed at 2,000 psi for 5 min to produce a pellet for analysis. The wavenumber ranges from 400 cm^{-1} to 4,000 cm^{-1}. Raman spectroscopic measurements were carried out using a Renishaw Raman Microprobe (Type RM-1000), with a laser (514.5 nm) excitation source having a power at the specimen of the order of 2.5 mW. The (Charge Coupled Device) CCD exposure time was 30 s and every sample scanned 10 times. Raman spectra

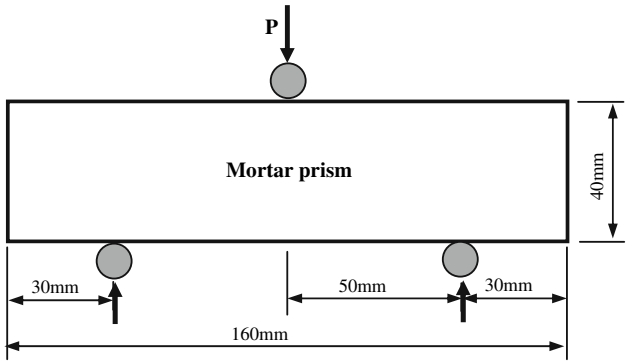

Fig. 1 Schematic diagram of the flexural strength test

data were generated from 200 cm^{-1} to 1,500 cm^{-1} in 2 cm^{-1} increments. A JEOL SX-4 scanning electron microscope (SEM) was used and the accelerating voltage was maintained at 20 kV. Samples were coated with a thin film of gold before testing.

3. Results and Discussion

3.1 Visual Inspection

A visual inspection of the mortar specimens was carried out monthly. After the initial 27 day curing under water, a little of white precipitate was present in the sample containers, particularly on the top surface of the specimens. This material is attributed to the CH leaching-out from the mortar and a little of carbonate in water. With the increasing curing under water, the precipitate accumulates continuously, and a white powdery coating formed on the whole top surface and partial side surface of the control specimens when immersed for 1 year. However, storage in water appeared to be benign, no evidence of cracking and spalling was detected on the control samples during the whole experiment.

Expect for some white materials covering the surface and filling the coarse pores, no other visual degradation occurred on the mortars immersed in sulfate solutions during the first 4 months. After 6 months storage, some signs of deterioration were first found on the surfaces and edges of the specimens exposed to the solutions containing magnesium sulfate, and there is no distinct difference among the specimens at different temperatures. A longer time of 7 months was required for the specimens stored in sodium sulfate solutions when visible sign of attack were first observed on the specimen surfaces. In all cases, the first sign of attack was the deterioration of the corners followed by cracking along the edges. Progressively, expansion and spalling took place on the surface of the specimens.

Figure 2 shows the visual appearances of specimens after 1 year exposure to different sulfate solutions. Obvious signs of deterioration were observed in all specimens, presenting extensive spalling and cracking on the surfaces. A white soft substance formed in the surface cracks and under the falling hard layer. From the visual inspection, it was found that magnesium sulfate solutions resulted in much severer deterioration of the mortars than sodium sulfate solutions. When exposed to the same magnesium sulfate solutions, the mortars at temperature of 20 °C and cycling temperature of 5 °C and 20 °C were more greatly damaged than the mortars at 5 °C. On

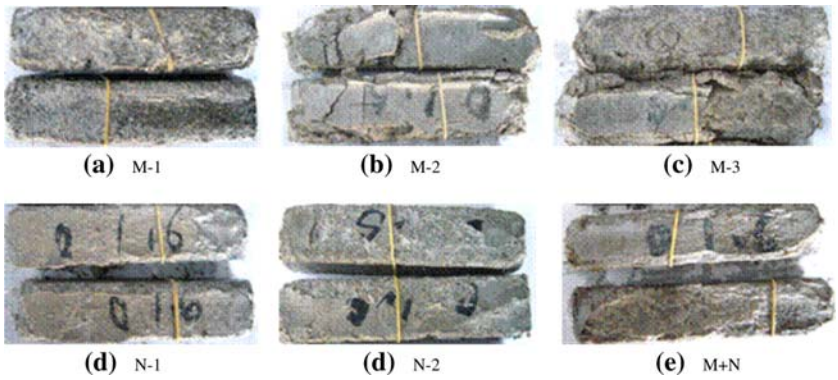

Fig. 2 Visual appearance of specimens after exposure to different sulfate environments for 1 year

Table 3 Compressive, σ_c (MPa), and flexural, σ_f (MPa), strength development of the control mortar specimens (stored in water) after initial 28 days curing

Time (days)	0	120	210	300	360
σ_c (Mpa)	47.7	53.2	54.7	54.3	54.5
σ_f (Mpa)	8.5	10.0	10.5	10.3	10.5

the basis of only the visual appearances, it cannot be found that temperature has an apparent effect on sulfate attack of mortars exposed to sodium sulfate solutions. When stored at the same temperature 5 °C, the mortars suffered more degradation in 2% Na_2SO_4, 2% $MgSO_4$, and 2% $MgSO_4$ + 2% Na_2SO_4 solutions, in ascending order.

3.2 Strength Development

Table 3 shows that the compressive and flexural strength of the control specimens increased steadily during the first 210 days storage in water (after the initial 28 day curing), and then it varied slightly. This may be attributed to the continued hydration of the cement at a degressive speed and a little negative influence of the CH leaching during a long-term water curing.

The strength development of mortar specimens immersed in different sulfate solutions is shown in Fig. 3. It is seen that the mortar presented a significant loss of strength after a long-time exposure to sulfate solutions under various conditions. With the increasing time of exposure to sulfate solutions, the strength loss of mortars increased evidently. When exposed to $MgSO_4$ solutions, the mortar got the most strength loss at 20 °C, the least strength loss at 5 °C and the medium strength loss at cycling temperatures of 5 °C and 20 °C. In the case of Na_2SO_4 solutions, the difference of temperatures had an insignificant influence on the strength loss of mortars. At the same temperature of 5 °C, the mortars in 2% Na_2SO_4 + 2% $MgSO_4$ solution suffered the most strength loss, and the mortars in 2% Na_2SO_4 solution had the least strength loss. These results are consistent with the above visual inspection.

Therefore it is indicated that the relative aggressiveness of the sulfate solutions at 5 °C used in this study is outlined below, from least aggressive to most aggressive: 2% Na_2SO_4, 2% $MgSO_4$, 2% Na_2SO_4 + 2% $MgSO_4$. A higher storage temperature seems to accelerate the degradation of limestone filler cement mortar exposed in sulfate solutions, with higher degragation for magnesium sulfate than sodium sulfate.

3.3 Mineralogy

The samples were selected from the surface of mortar prisms after 1 year exposure into different sulfate solutions. XRD patterns of them are shown in Fig. 4 (2θ from 8 to 40°). In all samples, there are strong peaks corresponding to quartz (SiO_2) from the sand and calcite ($CaCO_3$) from the limestone filler. Due to sulfate attack, only a small amount of portlandite ($Ca(OH)_2$) can be found in the samples, and even no detectable trace of portlandite can be seen in the M2 and M3 samples which means a severer deterioration of the mortars. At the same time, a great deal of sulfate-bearing substances including ettringite/thaumasite and gypsum formed in the attacked mortars.

Because ettringite and thaumasite have similar crystal structures, their XRD patterns show similarities (Ref 14) at the two major peaks at around 9.1 and 16.0° 2θ, it can be difficult to distinguish them when only small amounts are present, particularly if both may be present in a sample. However, some small peaks of the thaumasite at around 19.3, 23.3, and 28.0° 2θ are absent from the ettringite pattern. Likewise, there are prominent ettringite peaks that have no equivalent in the thaumasite pattern (e.g., at 22.9° 2θ). Accordingly, it can be found that both thaumasite and ettringite form in the mortars exposed to $MgSO_4$ and Na_2SO_4 + $MgSO_4$ solutions, while ettringite with a little thaumasite can be found in the XRD patterns of mortars exposed to Na_2SO_4 solutions. Strong peaks at 11.6° 2θ indicate the presence of gypsum in all the mortars exposed to the solutions containing Mg^{2+}. A little brucite ($Mg(OH)_2$, 18.6 and 38.0° 2θ) and greater quantities of gypsum can be found in the mortars in $MgSO_4$ solutions M-2 and M-3 with higher temperatures.

To obtain further evidence to corroborate these observations from XRD, further investigation was made using FTIR spectroscopy and Raman spectroscopy. The FTIR spectra of the same samples as in the XRD measurement are shown in Fig. 5. According to the previously published document (Ref 15), the obvious peaks at 501 cm^{-1} and 669 cm^{-1}, which were detected in all the mortars exposed to solutions containing $MgSO_4$, are assigned to the presence of SiO_6 bonds. Octahedral Si is such an extremely rare coordination state for mineral silicates that the presence of these two peaks indicates the formation of thaumasite or a thaumasite-containing solid solution. As indicated in the XRD pattern, the FTIR spectra show that just a little thaumasite formed in the mortars exposed to Na_2SO_4 solutions. The strong peaks at around 1,110 cm^{-1}

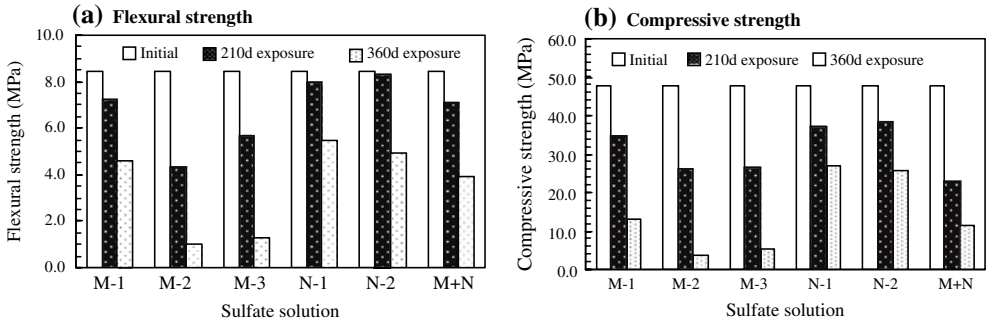

Fig. 3 Strength development of the mortars exposed to different sulfate solutions

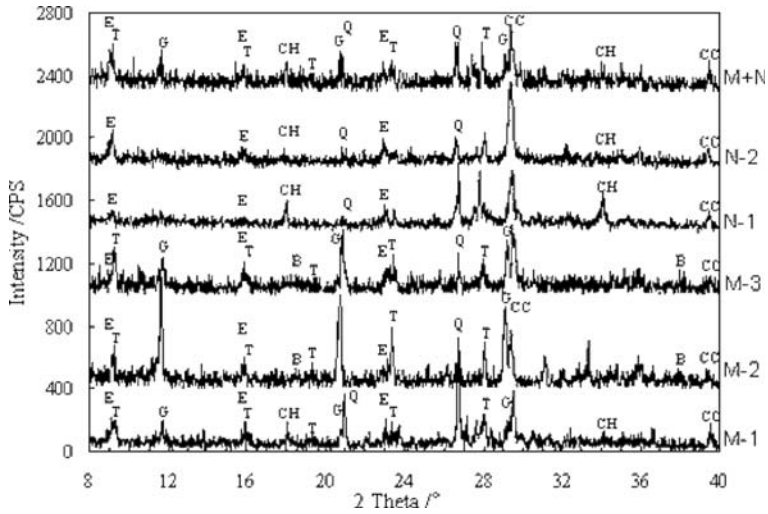

Fig. 4 XRD patterns of the mortar prisms after 1 year exposure to different sulfate solutions

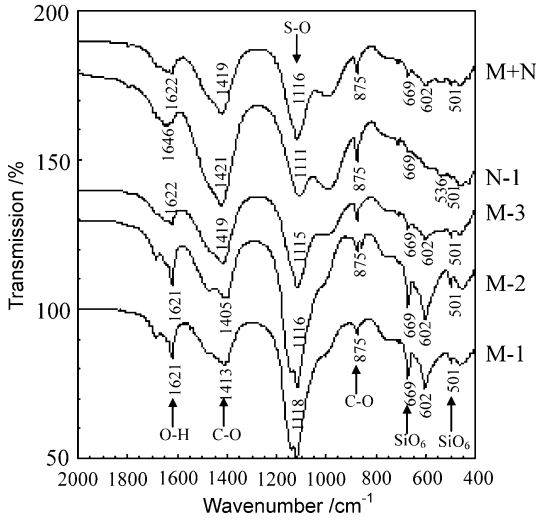

Fig. 5 FTIR spectra of limestone filler cement mortars after exposure to different sulfate environments for 1 year

associated with S-O show that a great deal of sulfate-bearing substances formed in all samples. The S-O peaks are stronger in the mortars exposed to solutions containing $MgSO_4$, showing that these mortars suffer severe attacks. Figure 6 presents Raman spectra of the deteriorated mortars after 1 year exposure to $MgSO_4$ solutions at 5 °C and 20 °C. The peaks at around 657 cm^{-1}, 988 cm^{-1}, and 1070 cm^{-1} are respectively attributed to Si-OH, sulfate, and carbonate groups of thaumasite. It can be adequately demonstrated that thaumasite forms in the two mortars exposed to sulfate solutions at both 5 °C and 20 °C.

The damaged mortar exposed to $MgSO_4$ solutions at 5 °C was selected as an example to observe the microstructure of deterioration products, and the SEM images are shown in Fig. 7. No CH crystal exists in the sulfate attacked mortar, and many club-shaped or needle crystals embedded irregularly in the pulpy material with a very open microstructure. Fig. 7(a) shows a large number of needle thaumasite crystals, smaller than 0.5 μm in diameter and 3-4 μm in length, covering the mortar surface. In the pores or surface cracks, there are many club-shaped gypsum crystals which have much larger sizes than thaumasite as shown in Fig. 7(b). The formation of both thaumasite and gypsum leads to the cracking, spalling, and decomposition of limestone filler cement mortar exposed to sulfate environment.

4. Discussion

From the visual observations and strength measurements reported in section 3.1 and 3.2, it can be clearly found that the

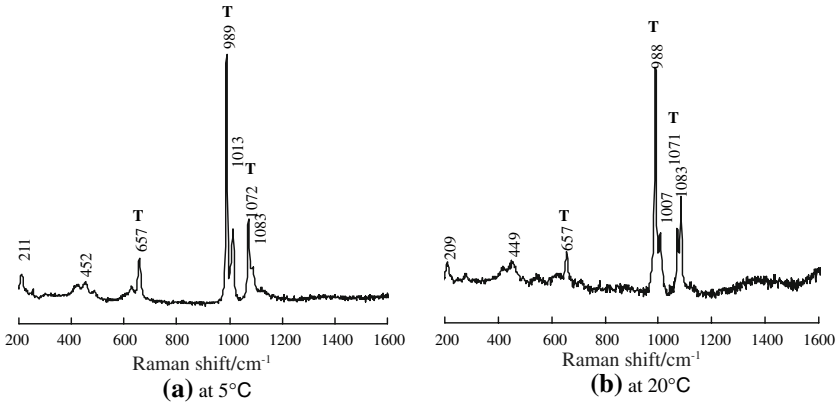

Fig. 6 Raman spectra of the deteriorated mortars after exposure to magnesium sulfate solutions for 1 year

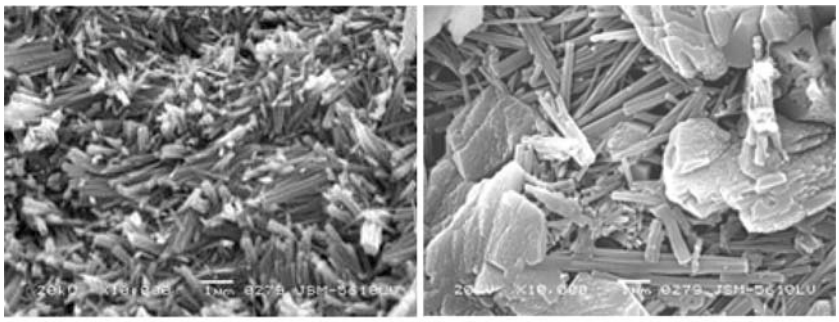

Fig. 7 SEM photos of the deteriorated mortar after exposure to magnesium sulfate solutions at 5 °C for 1 year

mortars deteriorated worse after 1 year storage in $MgSO_4$ solutions than in Na_2SO_4 solutions. Several researchers (Ref 7, 16) have reported that Mg^{2+} ions play a greatly detrimental effect in the sulfate attack of cements and concretes. First, magnesium sulfate can react with CH in the mortar to produce both gypsum and brucite, $Mg(OH)_2$, a sparingly soluble salt whose saturated solution has a pH of about 10.5. Once the available CH is depleted, the pH of the pore solution gets lowered. In this experiment, the sulfate solutions were replaced every 2 months and the measurements show that the pH value was about 9.5-10.0 in all the replaced Mg-containing solutions and remained above 12.5 in the replaced sodium sulfate solutions. This low pH of Mg-containing solution leads to the decalcification and breakdown of the C-S-H, whose stability requires a pH of about 12.5, to release more CH which reacts to form more brucite and gypsum, causing further decomposition of the C-S-H and the loss of the cementitious structure. In the advanced stages of attack, the Ca ion in the C-S-H can be completely replaced by the Mg ion, leading to the formation of magnesium silicate hydrate (M-S-H), which has been reported to be noncementitious (Ref 17). Continuous attack ultimately results in a severe degradation and strength loss of the mortar. Second, the decalcification and breakdown of C-S-H decreases the resistance of the mortar to ingress of magnesium sulfate, and it provides the silica to favor the thaumasite formation in mortar containing limestone filler. The XRD and FTIR data also present that storage in solutions containing $MgSO_4$ results in the formation of thaumasite near the surface of mortars, but only a little thaumasite can be found in the mortars immersed in Na_2SO_4 solutions. So it is suggested that magnesium ions also play a reinforcing influence on thaumasite sulfate attack. Third, with the same 2% mass concentration, $MgSO_4$ solution contains a higher concentration of SO_4^{2-} (16,000 ppm), to form more sulfate-bearing products, than Na_2SO_4 solution (13,700 ppm SO_4^{2-}). Therefore, the $MgSO_4$ solutions show more aggressive than the Na_2SO_4 solutions.

Most researchers (Ref 18, 19) believe that thaumasite forms below 15 °C, especially at about 10 °C or less, ideally within the range 0-5 °C under cold damp conditions. This viewpoint has also been supported by many field occurrences of thaumasite form of sulfate attack in UK, Italy, Germany, and Canada. Bensted (Ref 20) even suggested that thaumasite formation reaction does not occur to any perceptible extent at about 20 °C or above. In the report from the Thaumasite Expert Group (TEG), it is advised that 'Fairly low temperatures, generally less than 15 °C, are needed for vigorous formation of thaumasite' (Ref 21). Thus, 15 °C has been often regarded as the upper threshold for determining the thaumasite sulfate attack in practice. However, Diamond (Ref 10) reported that significant contents of thaumasite have been found in a building located in Southern California, a region with mild temperatures. Irassar (Ref 11) found that thaumasite occurred, near the surface of OPC + 20% limestone filler mortars, as the final stage of sulfate attack at (20 ± 2 °C). XRD, FTIR, and Raman analyses presented here on samples near the surface of OPC + 30% limestone filler mortars indicate the formation of

thaumasite after 1 year exposure to sulfate solutions at three different temperatures. It reveals that the formation of thaumasite is not limited to low temperature, and the thaumasite form of sulfate attack may affect a broader range of structures than expected.

Kleber's rule (Ref 22) suggests that an increase in temperature leads to a decrease in the formation of thaumasite because SiO_6 bond is ready to form at lower temperatures. Collett (Ref 23) presents that the increasing solubility of carbon dioxide must be one of the main reasons why thaumasite forms more readily at lower temperatures. But other researchers (Ref 24) and the above analysis results show that the decalcification of C-S-H, under magnesium sulfate attack, also favors the thaumasite formation through releasing the silica. In this experiment, it is not easy to determine the effect of temperatures on the amount of thaumasite formed in the attacked mortars. Further investigations are needed for such a quantitative analysis. According to Santhanam (Ref 25), an increase in the temperature of the attacking solution causes the rate of diffusion to increase. Divet (Ref 26) observes that higher temperature leads to more adsorption of the SO_4^{2-} ions on the surface of C-S-H. Hence, the formation of gypsum, ettringite, and brucite, the depletion of CH and the decalcification and decomposition of C-S-H would be accelerated when the temperature is increased. The occurrence of more such crystal phases has been confirmed by the XRD analysis in section 3.3. At early stages, the ettringite formation leads to surface cracking, and later stages when the pH drops to below 10.5, the gypsum formation becomes the main resource of swelling and cracking which develops from the outer surface to the interior part of mortar. On the other hand, the decomposition of C-S-H reduces the strength of mortar greatly, and it looses the silica to form thaumasite which accelerates the strength loss further. Thus, the overall deterioration of the mortar, due to a severer traditional sulfate attack accompanied by thaumasite form of sulfate attack, becomes worse with increasing temperature.

5. Conclusions

From the present study, the following conclusions can be drawn:

- The relative aggressiveness of sulfate solutions at 5 °C used in this study is outlined below, from most aggressive to least aggressive: 2% Na_2SO_4 + 2% $MgSO_4$ > 2% $MgSO_4$ > 2% Na_2SO_4.
- The increase of solution temperature accelerates both magnesium attack and sulfate attack on the limestone filler cement mortar, and leads to more deleterious products including gypsum, ettringite, and brucite formed on the surface of mortars after 1 year storage in sulfate solutions. The overall deterioration of mortars gets worse at a higher temperature when excessive water and sulfates exist.
- Mg^{2+} ions reinforce the thaumasite sulfate attack on the limestone filler cement mortars. Thaumasite forms in the mortars containing limestone filler after exposure to magnesium sulfate solutions at both 5 °C and 20 °C. It reveals that the thaumasite form of sulfate attack is not limited to structures at low temperatures.

Acknowledgments

This work is funded by National Natural Science Foundation of China (No.50408016) and the 863 High-Tech Research and Development Program of China (No.2005AA332010).

References

1. P. Poitevin, Limestone Aggregate Concrete, Usefulness and Durability, *Cem. Concr. Compos.*, 1999, **21**(2), p 89–97
2. S. Tsivilis, J. Tsantilas, G. Kakali, E. Chaniotakis, and A. Sakellariou, The Permeability of Portland Limestone Cement Concrete, *Cem. Concr. Res.*, 2003, **33**(9), p 1465–1471
3. B.B. Violeta, SCC Mixes with Poorly Graded Aggregate and High Volume of Limestone Filler, *Cem. Concr. Res.*, 2003, **33**(9), p 1279–1286
4. S. Tsivilis, E. Chaniotakis, E. Badogiannis, G. Pahoulas, and A. Ilias, A Study on the Parameters Affecting the Properties of Portland Limestone Cements, *Cem. Concr. Compos.*, 1999, **21**(2), p 107–116
5. J. Baron and C. Dourve, Technical and Economical Aspects of the Use of Limestone Filler Additions in Cement, *World Cem.*, 1987, **18**, p 100–104
6. A.P. Barker and D.W. Hobbs, Performance of Portland Limestone Cements in Mortar Prisms Immersed in Sulfate Solutions at 5°C, *Cem. Concr. Compos.*, 1999, **21**(2), p 129–137
7. S.A. Hartshorn, J.H. Sharp, and R.N. Swamy, Thaumasite Formation in Portland-limestone Cement Pastes, *Cem. Concr. Res.*, 1999, **29**(8), p 1331–1340
8. M.E. Gaze and N.J. Crammond, The Formation of Thaumasite in a Cement:lime:sand Mortar Exposed to Cold Magnesium and Potassium Sulfate Solutions, *Cem. Concr. Compos.*, 2000, **22**(3), p 209–222
9. D.W. Hobbs and M.G. Taylor, Nature of the Thaumasite Sulfate Attack Mechanism in Field Concrete, *Cem. Concr. Res.*, 2000, **30**(4), p 529–533
10. S. Diamond, Thaumasite in Orange County, Southern California: An Inquiry into the Effect of Low Temperature, *Cem. Concr. Compos.*, 2003, **25**(8), p 1161–1164
11. E.F. Irassar, V.L. Bonavetti, M.A. Trezza, and M.A. González, Thaumasite Formation in Limestone Filler Cements Exposed to Sodium Sulphate Solution at 20°C, *Cem. Concr. Compos.*, 2005, **27**(1), p 77–84
12. M. Romer, L. Holzer, and M. Pfiffner, Swiss Tunnel Structures: Concrete Damage by Formation of Thaumasite, *Cem. Concr. Compos.*, 2003, **25**(8), p 1111–1117
13. N.J. Crammond and P.J. Nixon, Deterioration of Concrete Foundation Piles as a Result of Thaumasite Formation, Sixth International Conference on The Durability of Building Materials and Components, Oct 26-29, 1993 (Omiya, Japan), p 295–305
14. S.M. Torres, J.H. Sharp, R.N. Swamy, C.J. Lynsdal, and S.A. Huntley, Long Term Durability of Portland- limestone Cement Mortars Exposed to Magnesium Sulfate Attack, *Cem. Concr. Compos.*, 2003, **25**(8), p 947–954
15. J. Bensted and S.P. Varma, Studies of Thaumasite – Part II, Silicates Industrials, 39(1), 1974, p 11–19
16. Rasheeduzzafar, O.S.B. Al-Amoudi, S.N. Abduljauwad, and M. Maslehuddin, Magnesium-Sodium Sulfate Attack in Plain and Blended Cements, *ASCE J. Mater. Civil Eng.*, 1994, **6**(2), p 201–222
17. D. Bonen, Composition and Appearance of Magnesium Silicate Hydrate and its Relation to Deterioration of Cement Based Materials, *J. Am. Ceram. Soc.*, 1992, **75**(10), p 2904–2906
18. S.A. Hartshorn and I. Sims, Thaumasite, a Brief Guide for Engineers, *Concrete*, 1998, **32**(8), p 24–27
19. N. Crammond, The Occurrence of Thaumasite in Modern Construction—a Review, *Cem. Concr. Compos.*, 2002, **24**(4), p 393–402
20. J. Bensted, Thaumasite — Background and Nature in Deterioration of Cements, Mortars and Concretes, *Cem. Concr. Compos.*, 1999, **21**(2), p 117–121
21. Thaumasite Expert Group, The Thaumasite Form of Sulfate Attack: Risks, Diagnosis, Remedial Works and Guidance on New Construction, Department of the Environment, Transport and the Regions, London, 1999
22. A.R Brough and A. Atkinson, Micro-Raman Spectroscopy of Thaumasite, *Cem. Concr. Res.*, 2001, **31**(3), p 421–424

23. G. Collett, N.J. Crammond, R.N. Swamy, and J.H. Sharp, The Role of Carbon Dioxide in the Formation of Thaumasite, *Cem. Concr. Res.*, 2004, **34**(9), p 1599–1612
24. E.F. Irassar, V.L. Bonavetti, and M. González, Microstructural Study of Sulfate Attack on Ordinary and Limestone Portland Cements at Ambient Temperature, *Cem. Concr. Res.*, 2003, **33**(1), p 31–41
25. M. Santhanam, M.D. Cohenb, and J. Olek, Mechanism of Sulfate Attack: a Fresh Look Part 2. Proposed Mechanisms, *Cem. Concr. Res.*, 2003, **33**(3), p 341–346
26. L. Divet and R. Randriambololona, Delayed Ettringite Formation: the Effect of Temperature and Basicity on the Interaction of Sulphate and C-S-H Phase, *Cem. Concr. Res.*, 1998, **28**(3), p 357–363